$Li_{14}P_2O_2N_6$: Computational study of a possible new electrolyte for Li ion batteries

Ahmad Al-Qawasmeh and N. A. W. Holzwarth

Department of Physics, Wake Forest University, Winston-Salem, NC, USA

Introduction

Twenty-five years after the pioneering work at Oak Ridge National Laboratory on LiPON solid electrolytes[1–9], new lithium oxonitridophosphate continue to be discovered. LiPON materials have the stoichiometry $Li_xPO_yN_z$ with $x = 2y+3z-5$. The building blocks of these materials are the PO_uN_{4-u} tetrahedra which are often formed into dimers, trimers, infinite chains, or more complicated interconnections. Recently, Baumann and Schnick[10] found an interesting new crystalline LiPON which has the stoichiometry $Li_{14}P_2O_3N_6$ formed with a trigonal arrangement of isolated tetrahedral $(PON_3)^{-6}$ ions stabilized by isolated O^{-2} ions. We report the results of our computationally study of the bulk and interface structures and Li ion migration properties of $Li_{14}P_2O_3N_6$ in comparison with other LiPON materials also formed from arrangements of isolated oxonitridophosphate tetrahedra such as Li_7PN_4 and Li_3PO_4[11,12].

Calculational Methods

The computational methods used in this work are based on density functional theory (DFT)[13,14], using the projected augmented wave (PAW)[15] formalism. The PAW basis and projector functions were generated by the ATOMPAW[16] code and the crystalline materials were modeled using the QUANTUM ESPRESSO[17] package. Visualizations were constructed using the *XCrySDEN*,[18] *VESTA*[19] software packages.

The exchange correlation function is approximated using the local-density approximation (LDA)[20]. The choice of LDA functional was made based on previous investigations[21,22] of similar materials which showed that the simulations are in good agreement with experiment, especially the fractional lattice parameters, the vibrational frequencies, and heats of formation. The simulated magnitudes of the lattice parameters, when systematically scaled by a factor of 1.02, are also in good agreement with experiment.

The calculations were well converged with plane wave expansions of the wave function including $|\mathbf{k}+\mathbf{G}|^2 \leq 64$ bohr^{-2}. The Brillouin zone integrals were evaluated by using uniform sampling volumes of 0.006 bohr^{-3} or smaller. Convergence tests showed that increasing the sampling grid by a factor of 8 changed the total energy by less than 0.001 eV for 100 atom supercells. The partial densities of states were calculated as described in previous work[23], using weighting factors based on the charge within the augmentation spheres of each atom with radii $r_c^{\rm Li} = 1.6$, $r_c^{\rm P} = 1.7$, $r_c^{\rm O} = 1.2$, and $r_c^{\rm N} = 1.2$ in bohr units. The reported partial densities of states curves $\langle N^a(E)\rangle$ were averaged over the atomic sites of each type a.

Simulation of Li ion migration were performed at constant volume in supercells constructed from the op- timized conventional cells. In modeling charged defects (Li ion vacancies or interstitials), the system was assumed to remain electrically insulating and a uniform background charge was added in order to evaluate the electrostatic interactions. The minimum energy path for Li ion migration was estimated using the "nudged elastic band" (NEB) method[24] as programmed in the QUANTUM ESPRESSO package, using 5 images between each metastable configuration.

WAKE FOREST UNIVERSITY

Structure of the bulk material

Baumann and Schnick[10] reported the synthesis of $Li_{14}P_2O_3N_6$ by heating powders of $PO(NH_2)_3$ and $LiNH_2$ in a sealed silica glass ampoule for 24 hours at a temperature of 550 deg. C. The resulting crystals have a trigonal structure characterized by the space group $P\bar{3}$ (No. 147 as listed in the International Table of Crystallography). Figure [1] shows a ball and stick diagram of the structure from two different perspectives. The scale factor of 1.02 used to correct the systematic error on the magnitudes of the lattice constants due to the LDA functional puts the simulated lattice constants within 0.1 Å of the experimental results. The simulated fractional coordinates for the P, O, and N sites are all within 0.01 of the experimental results. For the Li sites, the simulated fractional coordinates differ from the experimental values by a larger amount (0.06 or less). It is our experience[25] that it is common to find that X-ray analysis is less sensitive to the the Li positions than to the positions of the other elements in the crystal which have larger X-ray cross sections due to their larger atomic numbers Z.

Simulations show that the trigonal symmetry is stabilized by the isolated O^{-2} ions located at the $1b$ sites and the corresponding Li^{+} ions located at the $2c$ sites. In addition to its trigonal symmetry, the crystal structure features an interesting arrangement of pairs of PON_3 tetrahedra, forming alternating c-axis planes of O^{-2} and N^{-3} ions. The arrangement of the isolated oxonitridophosphate tetrahedra is quite different from other crystalline LiPON materials of this type such as $\beta-$ and $\gamma-Li_3PO_4$ which has been studied previously[26,27] and Li_7PN_4[28,29].

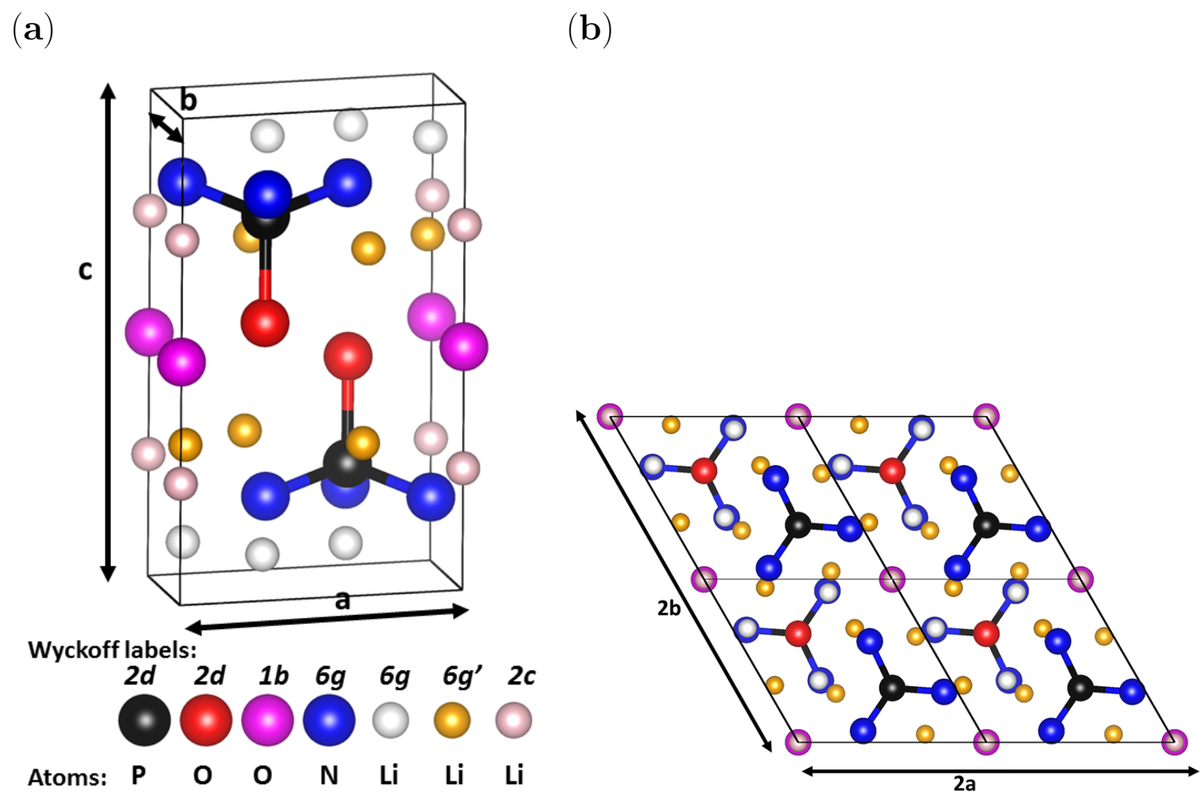

Fig [1]. (a) Ball and stick diagram of the $P\bar{3}$ structure of a unit cell of $Li_{14}P_2O_3N_6$, viewing the **c**-axis along the vertical direction, using the indicated ball conventions to distinguish the inequivalent sites, labeled according to their Wyckoff letters. (b) Projection of 4 unit cells of $Li_{14}P_2O_3N_6$ perpendicular to the **c** axis to show the trigonal symmetry.

WAKE FOREST UNIVERSITY

Electonic Structure of the bulk materials

It is interesting to compare the electronic structure of $Li_{14}P_2O_3N_6$ with other oxonitridophophates composed of isolated tetrahedra and related materials. The corresponding partial densities of states are given in Fig [2]. The valence band states are characterized by the $2p$ states of O and N together with bonding combinations the the P $3s$ and $3p$ states while the conduction bands are characterized by the corresponding antibonding states. The N $2p$ states dominate the top of the valence band for $Li_{14}P_2O_3N_6$. The O $2p$ contributions to $Li_{14}P_2O_3N_6$ are of two types. The occupied states associated with P-O bonds contribute to the bottom of the valence band, while the non-bonded O $2p$ states contribute to the middle of the valence band. Knowing that LDA calculations typically underestimate band gaps, we can safely conclude that the four materials are good insulators, having band gaps larger than 3 eV.

Related to the electronic structure is the stability of the compounds relative to decomposition. These can be roughly estimated from the calculated total energies, assuming that vibrational energies including zero point energies can be neglected. For example, we considered the following possible decomposition reaction.

$$Li_{14}P_2O_3N_6 \rightarrow 3Li_2O + 2Li_3N + 2LiPN_2 - 2.92\text{eV}. \quad (1)$$

The negative energy on the right side of the equation indicates that $Li_{14}P_2O_3N_6$ is stable with respect to decomposition into these binary and ternary products. In anticipation of the study of interfaces of this electrolyte with Li metal, we also considered the energy associated with reaction with Li metal as follows.

$$Li_{14}P_2O_3N_6 + 16Li \rightarrow 3Li_2O + 6Li_3N + 2Li_3P + 3.1\text{eV}. \quad (2)$$

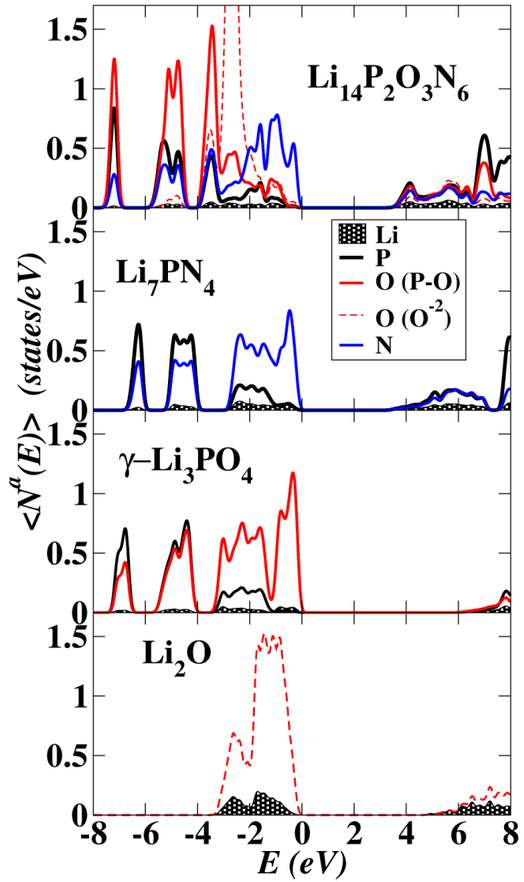

Fig [2] Partial density of states plot for the LiPON materials $Li_{14}P_2O_3N_6$ and Li_7PN_4 in comparison with γ-Li_3PO_4 and Li_2O. Oxygen contributions from isolated O^{-2} ions and from oxygens associated with P$-$O bonds are distinguished with dashed and full red lines, respectively. In each plot, $E = 0$ is aligned at the top of the valence band.

Li ion migration mechanisms in $Li_{14}P_2O_3N_6$

Li ion migration in $Li_{14}P_2O_3N_6$ was investigated using supercells based on $2 \times 2 \times 1$ multiples of the unit cell. .Table summarizes the 3 inequivalent vacancy energies relative to the g' site vacancy and 2 inequivalent interstitial energies relative to the I site interstitial. The placements of these defect sites are illustrated in Figs. [3a] and [3c] in an orthorhombic construction of the hexagonal unit cell.

Vacancies	
Multiplicity and Wyckoff Label	Relative Energy (eV)
$4g'$	0.00
$4g$	0.95
$2c$	0.41
Interstitials	
Fractional Coordinates	Relative Energy (eV)
$I \equiv$(13,23,0.73) ($2d$)	0.00
$II \equiv$(0, 0, 0) ($1a$)	0.22

In order to study likely migration pathways, using the NEB method[24], we considered a range of near neighbor hops between defect sites, the large range of the relative energies of the unique vacancy configurations listed in Table [1]. For the vaccancy mechanism four different paths were found as shown in figure [3a]. For the interstatial and the kick-out mechanism two paths were found as shown in figure [3c]. The coressponding migration energies for the vacancy and the kick-out mechanisms are shown in figure [3b] and [3d] recpectively. the NEB calculation shows that the fovorable conduction mechanism is the vacancy mechanism which takes place near the oxygen plane with E_m = 0.3 eV.

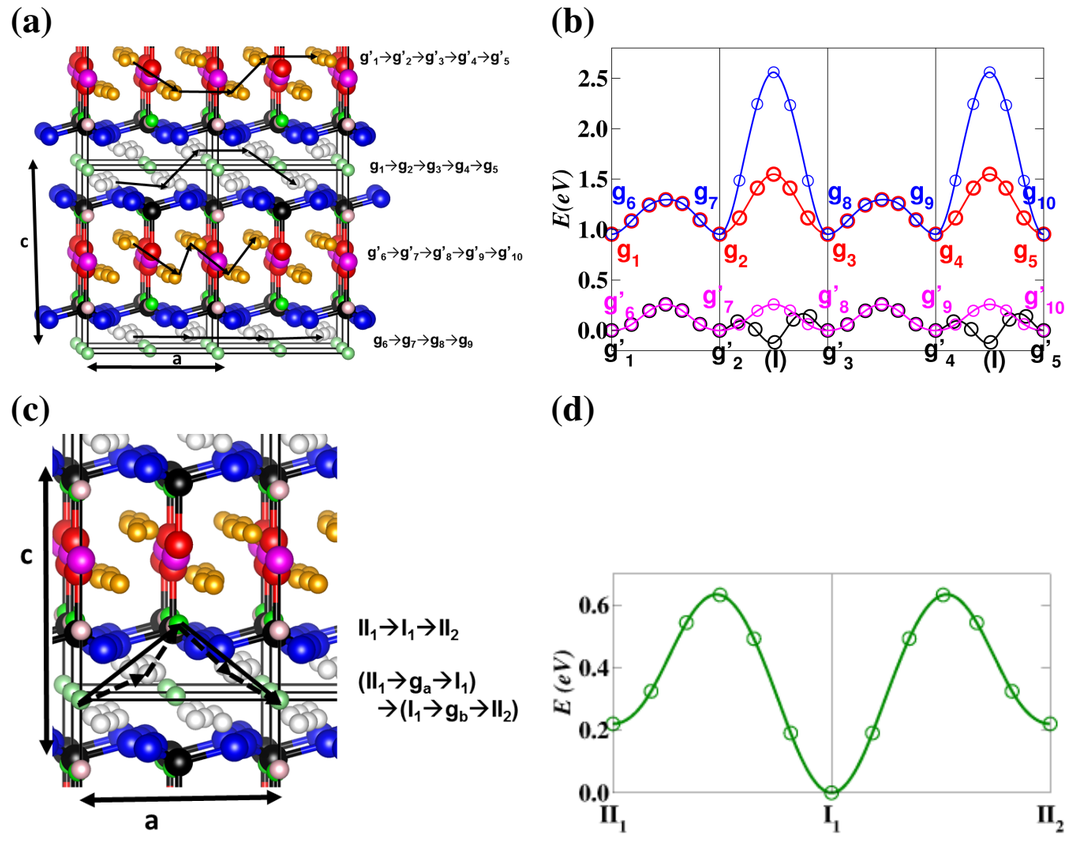

Fig [3] Panels (a) and (c) show ball and stick models of several supercells of $Li_{14}P_2O_3N_6$ using the same ball conventions as in Fig [1]. with the addition of type I and II interstitial sites shown in bright and pale green, respectively. The **a** and **c** axes are indicated in the diagrams while the third axis of the diagram is perpendicular to the other two, specifically constructed in the $\mathbf{a} + \mathbf{2b}$ direction. Panels (b) and (d) show energy path diagrams from NEB simulations of Li ion migration between metastable vacancy or interstitial configurations indicated by the vertical lines.

WAKE FOREST UNIVERSITY

Li electrolyte interface in $Li_{14}P_2O_3N_6$

We prepared two series of configurations of interfaces of $Li_{14}P_2O_3N_6$[c] with Li as shown in Fig 4 (a) and (b) and the corresponding plots of the surface energy versus the number of metallic lithium atoms n_b are evaluated as plotted in Fig [4c]. Interface configurations Ω_1 and Ω_2 have approximately the same density of the Li atoms per unit volume 0.05-0.06 atoms/Å^3, close to the density of bulk Li. The estimated strains of the two configurations are $\sigma(\Omega_1) = 0.0004$ eV/Å^2 and $\sigma(\Omega_2) = 0.0014$ eV/Å^2, consistent with the notion that the more regular structure of configuration Ω_1 produces smaller strain. The strain corrected interface energy, $\gamma_{ab}^{\lim}$, for the two configurations is found to be approximately 0.05 eV/Å^2. This value is similar to the corresponding values of 0.03-0.04 eV/Å^2 reported by Lepley[21] for interfaces of β- or γ- Li_3PO_4 with Li metal.

The partial densities of states for the interface Fig [4a] with $n_b = 36$ are shown in Fig [4d]. The partial densities of states for the interior of the electrolyte is very similar to that of the bulk structure of $Li_{14}P_2O_3N_6$ shown in Fig [2]. The metallic Li states are physically separated from the electrolyte, but energetically overlap with the top of the $Li_{14}P_2O_3N_6$ valence band by approximately 1 eV. The partial densities of states associated with the Li ions at the interface of the electrolyte and the metallic Li, show that they have more electronic charge than the Li^+ ions in the interior of the electrolyte. The "Electrolyte Li" curve in the top portion of the plot Fig [4d] is the same as the "Li" curve in lower portion of the plot representing ionic Li within the interior of the electrolyte. The "Interface Li". Also shown in the top portion of the plot Fig [4d] are the "Interface Li" contributions corresponding to Li sites nearest the electrolyte and the "Metallic Li" contributions corresponding to the interior of the metallic Li region of the supercell.

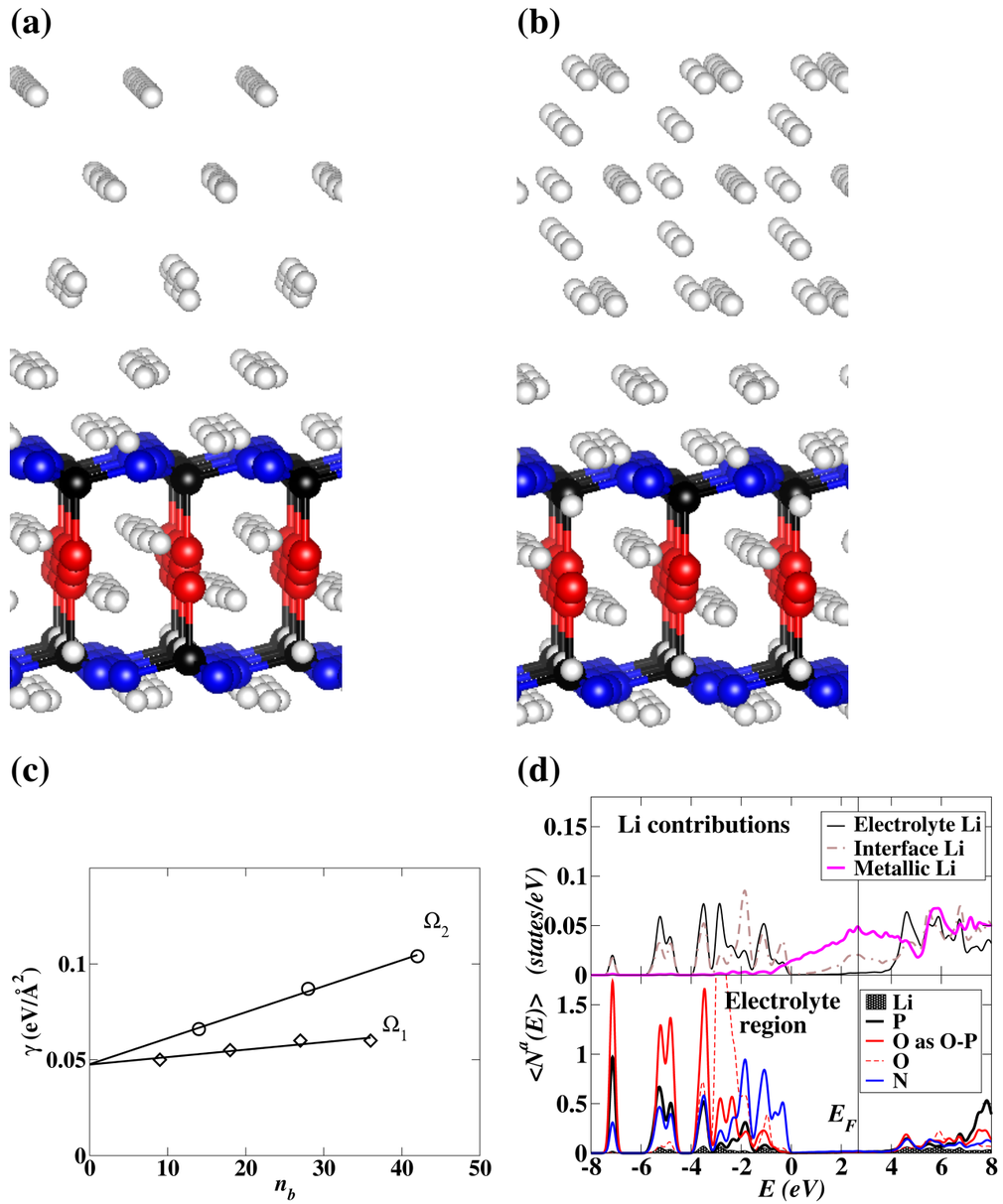

Fig [4]

Summary and Conclusions

The results of the reported simulations suggest that the nitrogen rich crystalline lithium oxonitridophosphate material of this study – $Li_{14}P_2O_3N_6$ – show promising properties as solid electrolyte for Li ion batteries, possibly for use with Li metal anodes.

Simulations of idealized interfaces constructed for $Li_{14}P_2O_3N_6$/Li is structurally metastable and electrically insulating. The partial densities of states associated with the interfaces show small effects in their electronic structures, while the partial densities of states associated with the interior of the electrolyte is identical to it bulk values. The partial densities of states associated with the metallic Li layers show that the Fermi level of the system lies well within the band gap of the interior layers of the electrolyte. While the total energy results for these LiPON electrolytes suggest exothermic reactions with Li under equilibrium conditions such as shown in Eq [2]. These simulations show that LiPON/Li interface are likely to be practically stable as has been shown in experimental demonstrations.

The simulations also suggest that the activation energies for Li ion migration in the nitrogen rich electrolyte is also quite promising. We found that the most efficient predicted activation energy for Li ion migration in $Li_{14}P_2O_3N_6$ is 0.3-0.4 eV for a pure vacancy mechanism involving g' site Li ions. The predicted activation energy for Li ion migration in $Li_{14}P_2O_3N_6$ is lower than the experimentally measured values for Li_7PN_4[31] and for γ-Li_3PO_4[32] as well as the $E_A = 0.6$ eV values measured for typical amorphous LiPON films.

Refrences

[1] N. J. Dudney, Thin film micro-batteries, Interface 17(3) (3) (2008) 44 48.

[2] J. B. Bates, N. J. Dudney, B. Neudecker, A. Ueda, C. D. Evans, Thin- film lithium and lithium-ion batteries, Solid State Ionics 135 (2000) 33 45.

[3] X. Yu, J. B. Bates, J. G. E. Jellison, F. X. Hart, A stable thin-film lithium electrolyte: Lithium phosphorus oxynitride, Journal of the Elec- trochemical Society 144 (1997) 524532

[4] B. Wang, B. C. Chakoumakos, B. C. Sales, B. S. Kwak, J. B. Bates, Synthesis, crystal structure, and ionic conductivity of a polycrystalline lithium phosphorus oxynitride with the -Li 3 PO 4 structure, Journal of Solid State Chemistry 115 (1995) 313323.

[5] J. B. Bates, N. J. Dudney, D. C. Lubben, G. R. Gruzalski, B. S. Kwak, X. Yu, R. A. Zuhr, Thin-film rechargeable lithium batteries, Journal of Power Sources 54 (1995) 5862.

[6] B. Wang, B. S. Kwak, B. C. Sales, J. B. Bates, Ionic conductivities and structure of lithium phosphorus oxynitride glasses, Journal of Non- Crystalline Solids 183 (1995) 297306.

[7] J. B. Bates, G. R. Gruzalski, N. J. Dudney, C. F. Luck, X. Yu, Recharge- able thin-film lithium batteries, Solid State Ionics 7071 (1994) 619628.

[8] J. B. Bates, N. J. Dudney, G. R. Gruzalski, R. A. Zuhr, A. Choudhury, D. F. Luck, J. D. Robertson, Fabrication and characterization of amor- phous lithium electrolyte thin films and rechargeable thin-film batteries, Journal of Power Sources 4344 (1993) 103110.

WAKE FOREST UNIVERSITY

[9] J. B. Bates, N. J. Dudney, G. R. Gruzalski, R. A. Zuhr, A. Choudhury, D. F. Luck, J. D. Robertson, Electrical properties of amorphous lithium electrolyte thin films, Solid State Ionics 5356 (1992) 647654.

[10] D. Baumann, W. Schnick, Li 14 (PON 3) 2 O - A Non-Condensed Oxonitridophosphate Oxide, European Journal of Inorganic Chemistry 2015 (4) (2015) 617621. doi:10.1002/ejic.201403125. URL http://doi.wiley.com/10.1002/

[11] Y. A. Du, N. A. W. Holzwarth, Li ion diffusion mechanisms in the crystalline electrolyte -Li 3 PO 4 , Journal of the Electrochemical Society 154 (2007) A999A1004.

[12] Y. A. Du, N. A. W. Holzwarth, Mechanisms of Li + diffusion in crystalline Li 3 PO 4 electrolytes from first principles, Phys. Rev. B 76 (2007) 174302 (14 pp).

[13] P. Hohenberg, W. Kohn, Inhomogeneous electron gas, Physical Review 136 (1964) B864B871.

[14] W. Kohn, L. J. Sham, Self-consistent equations including exchange and correlation effects, Physical Review 140 (1965) A1133A1138.

[15] P. E. Bl ochl, Projector augmented-wave method, Phys. Rev. B 50 (1994) 1795317979.

[16] N. A. W. Holzwarth, A. R. Tackett, G. E. Matthews, A Projector Augmented Wave (PAW) code for electronic structure calculations, Part I: atompaw for generating atom-centered functions, Computer Physics Communications 135 (2001) 329347, available from the website http://pwpaw.wfu.edu.

[17] P. Giannozzi, S. Baroni, N. Bonini, M. Calandra, R. Car, C. Cavaz- zoni, D. Ceresoli, G. L. Chiarotti, M. Cococcioni, I. Dabo, A. D. Corso, S. de Gironcoli, S. Fabris, G. Fratesi, R. Gebauer, U. Gerstmann, C. Gougoussis, A. Kokalj, M. Lazzeri, L. Martin-Samos, N. Marzari, F. Mauri, R. Mazzarello, S. Paolini, A. Pasquarello, L. Paulatto, C. Sbraccia, S. Scandolo, G. Sclauzero, A. P. Seitsonen, A. Smogunov, P. Umari, R. M. Wentzcovitch, Quantum espresso: a modular and open- source software project for quantum simulations of materials, J. Phys.: Condens. Matter 21 (39) (2009) 394402 (19pp), available from the web- site http://www.quantum-espresso.org.

[18] A. Kokalj,XCrySDen an new program for displaying crys- talline structures and densities, Journal of Molecular Graphics and Modelling 17 (1999) 176179, code available at the website http://www.xcrysden.org.

[19] K. Momma, F. Izumi, Vesta 3 for three-dimensional visualiza- tion of crystal, volumetric, an morphology data, Applied Crys- tallography 44 (2011) 12721276, code available from the website http://jp-minerals.org/vesta/en/.

[20] J. P. Perdew, Y. Wang, Accurate and simple analytic representation of the electron-gas correlation energy, Phys. Rev. B 45 (1992) 1324413249.

[21] Y. A. Du, N. A. W. Holzwarth, First-principles study of LiPON and related solid electrolytes, Phys. Rev. B 81 (2010) 184106 (15pp).

[22] K. Senevirathne, C. S. Day, M. D. Gross, A. Lachgar, N. A. W.

[23] N. D. Lepley, N. A. W. Holzwarth, Y. A. Du, Structures, Li+ mobilities, and interfacial properties of solid electrolytes Li_3 PS_4 and Li_3 PO_4 from first principles, Phys. Rev. B 88 (2013) 104103 (11 pp).

[24] H. J onsson, G. Mills, K. W. Jacobsen, Nudged elastic band method for finding minimum energy paths of transitions, in: B. J. Berne, G. Ci- ccotti, D. F. Coker (Eds.), Classical and Quantum Dynamics in Con- densed Phase Simulations, World Scientific, Singapore, 1998, pp. 385 404.

[25] A. Al-Qawasmeh, J. Howard, N. A. W. Holzwarth, Li_4SnS_4 and Li_4SnSe_4 : Simluations of Their Structure and Electrolyte Properties, J. Electrochem. Soc. 164 (2017) A6386A6394.

[26] Y. A. Du, N. A. W. Holzwarth, Effects of O vacancies and N or Si substitutions on Li + migration in Li 3 PO 4 electrolytes from first principles, Phys. Rev. B 78 (2008) 174301.

[27] N. A. W. Holzwarth, N. D. Lepley, Y. A. Du, Computer modeling of lithium phosphate and thiophosphate electrolyte materials, Journal of Power Sources 196 (2011) 68706876.

[28] W. Schnick, J. Luecke, Synthesis and crystal structure of lithium phos- phorus nitride Li_7 PN_4 : the first compound containing isolated PN_4 tetrahedra, Journal of Solid State Chemistry 37 (1990) 101106.

[29] W. Schnick, J. Luecke, Lithium ion conductivity of $LiPN_2$ and Li_7 PN_4 , Solid State Ionics 38 (1990) 271273.

[30] N. D. Lepley, N. A. W. Holzwarth, Modeling interfaces between solids: Application to li battery materials, Phys. Rev. B 92 (2015) 214201.

[31] W. Schnick, J. Luecke, Lithium ion conductivity of $LiPN_2$ and Li_7 PN_4 , Solid State Ionics 38 (1990) 271273.

[32] A. K. Ivanov-Shitz, V. V. Kireev, O. K. Melnikov, L. N. Demainets, Growth and ionic conductivity of -Li_3 PO_4 , Crystallography Reports 46 (2001) 864867.

Acknowledgements

This work was supported by NSF grant DMR-1507942. Computations were performed on the Wake Forest University DEAC cluster, a centrally managed resource with support provided in part by the University. We would also like to thank Dr. Nicholas Lepley for the use of his unpublished simula- tions of a -Li 3 PO 4 /Li interface.